# Does Aurophilicity Exist Beyond the Solid State?

# Supporting Information

Yury V. Vishnevskiy,[1,2,a] Felix Müller,[1] Ivan Y. Kurochkin,[3] A. Daniel Boese,[4] Raphael J. F. Berger,[5] Georgiy V. Girichev,[6] Norbert W. Mitzel[1,b]

[1] Lehrstuhl für Anorganische Chemie und Strukturchemie (ACS), Fakultät für Chemie, Universität Bielefeld, Universitätsstraße 25, 33615 Bielefeld, Germany

[2] Chemistry Department, Lomonosov Moscow State University, Leninskie Gory, 1/3, Moscow, 119991, Russia

[3] Institute of Microelectronics Technology RAS, 6 Academician Ossipyan str., 142432 Chernogolovka, Russia

[4] Department of Chemistry, University of Graz, 8010 Graz, Austria

[5] Chemistry and Physics of Materials, Paris-Lodron University Salzburg, Jakob-Haringer-Str. 2A, A-5020 Salzburg, Austria

[6] Department of Physics, Ivanovo State University of Chemistry and Technology, Sheremetevsky Ave. 7, 153000 Ivanovo, Russia

[a] E-mail: yury.vishnevskiy@uni-bielefeld.de

[b] E-mail: mitzel@uni-bielefeld.de

# Contents



# List of Tables



# List of Figures

# 1 Gas electron diffraction

Gas electron diffraction (GED) investigation has been performed in two stages: (1) measurements of diffraction patterns and (2) modeling and molecular structure refinements.

## 1.1 Experiments

The diffraction patterns for **3** were obtained in synchronous GED/MS experiments conducted with the EMR-100/APDM-1 apparatus[1–3] (Fig. S1). A stainless steel X18H10T effusion cell with a cylindrical effusion nozzle of 0.6×1.6 mm size (diameter×length) was used for the evaporation of samples. The ratio of the evaporation area to the effusion orifice area exceeded 400. The precise wavelengths of diffracted electrons were calibrated utilizing polycrystalline zinc oxide. The conditions of the GED/MS experiments are detailed in Table S1.

Table S1: Parameters of GED-MS experiments I and II.

| Parameter | I | II |
|---|---|---|
| $L^a$, mm | 598 | 338 |
| $N^b$ | 6 | 6 |
| $\lambda^c$, Å | 0.04285(4) | 0.04308(7) |
| $I^d$, $\eta$A | 1.04 | 1.4 |
| $T^e$, K | 503(2) | 508(1) |
| $\tau^f$, s | 60 | 81 |
| $s_{min}$–$s_{max}/\Delta s$ $^g$, Å$^{-1}$ | 1.2-15.3/0.1 | 2.3-27.6/0.1 |
| $U_{ion}{}^h$, V | 50 | 50 |
| $p_{col}{}^i$, Torr | $4.1{\cdot}10^{-6}$ | $1.8{\cdot}10^{-6}$ |
| $p_{MS}{}^j$, Torr | $1.0{\cdot}10^{-7}$ | $1.9{\cdot}10^{-7}$ |

$^a$ - Nozzle-to-plate distance. $^b$ - Number of recorded films. $^c$ - Wavelength of electrons. $^d$ - Primary electrons beam current. $^e$ - Temperature of effusion cell. $^f$ - Exposure time. $^g$ - Scattering angles range and step. $^h$ - Ionization voltage. $^i$ - Residual gas pressure in the diffraction chamber. $^j$ - Residual gas pressure in the mass-spectrometry block.

## 1.2 Structure refinements

A preliminary modeling of the possible conformers of **3** was undertaken using the semi-empirical method GFN2-xTB[4], implemented in the CREST 2.10.2 software[5–7]. It resulted

in a single stable conformation of $C_{2h}$ symmetry with planar $AuC_2PAuC_2P$ cycle.

Molecular structure of **3** has been refined using the UNEX program[8]. Starting molecular geometrical parameters were taken from PBE0-D3/cc-pVTZ(H,C,F,P);def2-QZVPP(Au).

Two sets of interatomic vibrational amplitudes and corrections have been tested, computed by (a) using perturbation theory and (b) from molecular dynamics (MD) trajectory. In the first case, harmonic and cubic force constants have been calculated at the PBE0-D3/cc-pVTZ(H,C,F,P);def2-QZVPP(Au) level of theory and processed by the VibModule program[9] implementing the Sipachev's first-order perturbation theory[10,11]. However, due to very small harmonic frequencies starting from 14 $cm^{-1}$ this theory were expected to be not enough accurate. Therefore it has been decided to follow an alternative way. For this, MD simulations have been performed using the i-PI program[12]. A path-integral (16 beads) NVT ($T$ = 508 K) simulation using PIGLET thermostat[13] has been done. The total collected trajectory length was 59.5 ps. It has been processed in UNEX for calculation of interatomic vibrational amplitudes and corrections (see Eqs. 2 - 3 in[14]) taking into account rotations of methyl groups and with control for the convergence. The obtained set of vibrational parameters of ED terms in **3** was considered as the most accurate and has been accepted for obtaining final results.

Refinement of parameters for **3** from ED data was performed in the frame of the least-squares (LS) method until the best fit of the tested model to the experimental molecular intensities has been achieved. Concisely, this procedure is expressed in the following equation:

$$\Phi_{\mathrm{GED}} = \sum_i (s_i M(s_i)_{\mathrm{exp}} - k_{\mathrm{M}} s_i M(s_i)_{\mathrm{theor}})^2 \rightarrow \min$$

where $s_i M(s_i)_{\mathrm{theor}}$ and $s_i M(s_i)_{\mathrm{exp}}$ are theoretical and experimental molecular scattering intensities; $s_i$ is reduced scattering angle, $k_{\mathrm{M}}$ is the scale factor.

The full set of variable parameters (Table S2) included 11 independent groups for **3**: 5 groups of bond lengths, 5 groups of bond angles, 1 group of dihedral angles.

Table S2: Full list of Z-matrix parameters of **3** sorted by groups

| | |
|---|---|
| | Bond lengths |
| + | $C_1$-$C_2$, $C_2$-$C_3$, $C_3$-$C_4$, $C_5$-$C_6$, $C_1$-$C_6$, $C_3$-F, $C_4$-F, $C_5$-F, $C_6$-F |
| + | Au-Au |
| + | Au-P, Au-C |
| + | P-$C_{Me}$ |
| + | $C_{Me}$-$H_1$, $C_{Me}$-$H_2$, $C_{Me}$-$H_3$ |
| | Bond angles |
| + | C-Au-P |
| + | P-Au-Au |
| + | C-P-$C_{Me}$ |
| + | $C_1$-$C_2$-$C_3$, $C_2$-$C_1$-$C_6$, $C_2$-$C_3$-$C_4$ |
| + | $C_2$-$C_3$-F, $C_1$-$C_6$-F, $C_3$-$C_4$-F, $C_6$-$C_5$-F |
| - | P-$C_{Me}$-$H_1$, P-$C_{Me}$-$H_2$, P-$C_{Me}$-$H_3$ |
| | Torsion angles |
| + | $C_{Me}$-P-Au-C |
| - | P-Au-Au-P, C-Au-Au-P |
| - | $C_1$-P-$C_2$-Au |
| - | $C_3$-$C_2$-$C_1$-Au |
| - | $C_3$-$C_2$-$C_1$-$C_6$, $C_1$-$C_2$-$C_3$-$C_4$ |
| - | $C_4$-$C_2$-$C_3$-F, $C_5$-$C_3$-$C_4$-F, $C_4$-$C_6$-$C_5$-F, $C_5$-$C_1$-$C_6$-F |
| - | $C_1$-P-$C_{Me}$-H, $C_1$-P-$C_{Me}$-H, $C_1$-P-$C_{Me}$-H |

"+" indicates that group was refined, "-" - indicates that group was fixed at the QC values. Atom numbers are shown in Fig. S2.

# 2 Mass spectra

Mass spectra of **3** were recorded during the GED/MS experiments on APDM-1 unit. Fig. S5 shows the averaged spectra obtained from two separate experiments, with the most intense peaks labeled. The mass spectra confirm the presence of molecular ions of the compound in the gas phase in sufficient quantity. Four groups of peaks were observed in the mass spectra (Fig. S5):

1) The molecular ion $[Au_2C_{16}H_{12}F_8P_2]^+$ with 812 Da, which is the most intensive in the spectrum, as well as the ion $[Au_2C_{16}H_{12}F_8P_2\text{-}CH_3]^+$ resulting from the detachment of one $CH_3$ group under electron impact in ionization chamber of MS.

2) From 600 to 680 Da region: correspond to different variants of ligand fragmentation again under electron impact in ionization chamber (detachment of $CH_3$ or $P(CH_3)_2$ groups

or $C_6H_4$ cycle or individual F atoms). The presence of two gold atoms in the ion structure is preserved.

3) From 360 to 480 Da region: the most intense peak in this region is the $[AuC_8H_6F_4P_2]^+$ ion with 406 Da, which is the result of the molecule splitting in half, including the Au-Au bond breaking. The remaining ions in this region arise from different variants of detachment of various ligand fragments under electron impact.

4) From 120 to 300 Da region: the most intense peaks in this region correspond to ions have more or less fragmented ligands that do not include Au atoms.

Traces of volatile impurities were observed in **3** at initial stages of GED experiments (Fig. S6). Total electron scattering intensity, sufficient for recording diffraction patterns, was achieved already at 398 K and was maintained when the temperature of the effusion cell increased up to 427 K. However, as the temperature increased, several molecular forms appeared, alternating with each other, first with mass numbers of 407-439 Da, then 477 Da. The impurity mass spectrum was joined by peaks of the compound **3** accompanied by a noticeable number of molecular forms with masses 845 and 878 Da at 477 K, which disappeared after a while at the same temperature. Further, only the target molecular form of **3** (812 Da) was present in vapour in scattering volume of GED. The confirmation of this statement and the absence of volatile admixtures in scattering volume of GED unit is the mass spectrum recorded at ionization voltage of 10 V containing the parent ion M+ only. The stable relative intensities of ions in mass spectra during whole period of recording the diffraction patterns for both nozzle-to-plate distances is the additional confirmation of presence in studied vapour the only molecular species, namely compound 3.

# 3 Quantum chemical calculations

HF[15,16], PBE0[17], B2PLYP[18], $\omega$B97X[19], PBEh-3c[20], r$^2$SCAN-3c[21], MP2[22] and SCS-MP2[23] calculations have been performed in Orca 6.1.1 program package[24,25]. Karlsruhe def2-

QZVPP basis sets[26] have been utilized, except for PBEh-3c and r$^2$SCAN-3c. In some cases empirical dispersion corrections D3[27], D3BJ[28] and D4[29] have been used. The target convergence in geometry optimizations has been set to *TightOpt*. The SCF convergence setting was at least *TightSCF* with grid *DefGrid3*. For all calculations the RIJCOSX[30–32] accelerating approximation has been turned on. With the same settings, an additional all-electron-correlated SCS-MP2 optimization has been done using the exact two-component theory (X2C)[33,34] paired with all-electron basis sets x2c-QZVPPall[35].

B3LYP[36,37], B97D[38], B98[39], BMK[40], PBE[41], BP86[42,43], CAM-B3LYP[44], LC-wPBE[45–47], M05[48], M06[49], M06HF[50,51], mPW1PW91[52], TPSSh[53,54], VSXC[55], X3LYP[56] calculations were performed in Gaussian 09[57] with the settings *Opt=Tight* and *grid=UltraFine*. B3LYP, PBE, BMK, BP86, CAM-B3LYP, LC-wPBE, M05, M06, and M06HF methods were used both with and without D3 dispersion corrections. Two combinations of basis set functions have been used: 1) cc-pVTZ to describe H, C, F, P atoms[58,59] and def2-QZVPP[26] for Au atoms; 2) def2-QZVPP for all atoms. Gold core electron shells were described by pseudopotentials in two variants: a) including into account relativistic effects - ECP60MWB[60] and without relativistic affects - ECP60MHF[61]. The basis sets were taken from the Basis Set Exchange software[62].

Potential energy along the Au...Au distance has been investigated in **3** at the CCSD(T) level of theory in its LNO-CCSD(T) variant[63,64] as implemented in the MRCC program package[65]. Extrapolation to the basis set limit has been used by employing aug'-cc-pV(T,Q)Z(-PP) basis sets[66–69] with the *vvtight* LNO criteria and aug'-cc-pV5Z(-PP) basis sets with the *tight* criteria, using diffuse functions on all atoms except hydrogen. The respective RI and RIJK basis sets have been taken from[70] and generated by an automatic generation procedure[71] respectively. Using this computational protocol the potential energy along the Au...Au distance has been scanned using the geometries obtained from RI-SCS-MP2(fc)/def2-TZVPP computations. Thus a rigid scan has been performed. At 2.82 Å and 2.83 Å for the Au...Au distance, our best estimates were 0.29 and 0.08 kJ/mol above the

minimum located approximately at 2.84 Å, whereas the potential remains rather flat towards larger distances, being 0.01 kJ/mol at 2.85 Å and 0.04 kJ/mol at 2.86 Å. We also investigated the effect of core electrons at the *vtight* LNO level using the aug'-cc-pwCVTZ(-PP) basis set when either correlating the core or only the valence electrons. This, however, only shifted the energy differences by less than 0.02 kJ/mol towards lower Au...Au distances. The LNO-CCSD(T) value at *vvTight* LNO thresholds and the basis set limit yields a minimum of energy for the Au...Au distance between 2.84 and 2.85 Å, while being a bit closer to 2.84 Å. However, it is to note that the potential energy surface at this region appears rather flat, especially when going towards larger Au...Au distances. At the final stage, energy corrections $\Delta E$(fc-SCS-MP2/def2-QZVPP - ae-X2C-SCS-MP2/x2c-QZVPPall) have been additionally utilized, which allowed to locate the minimum at 2.830 Å.

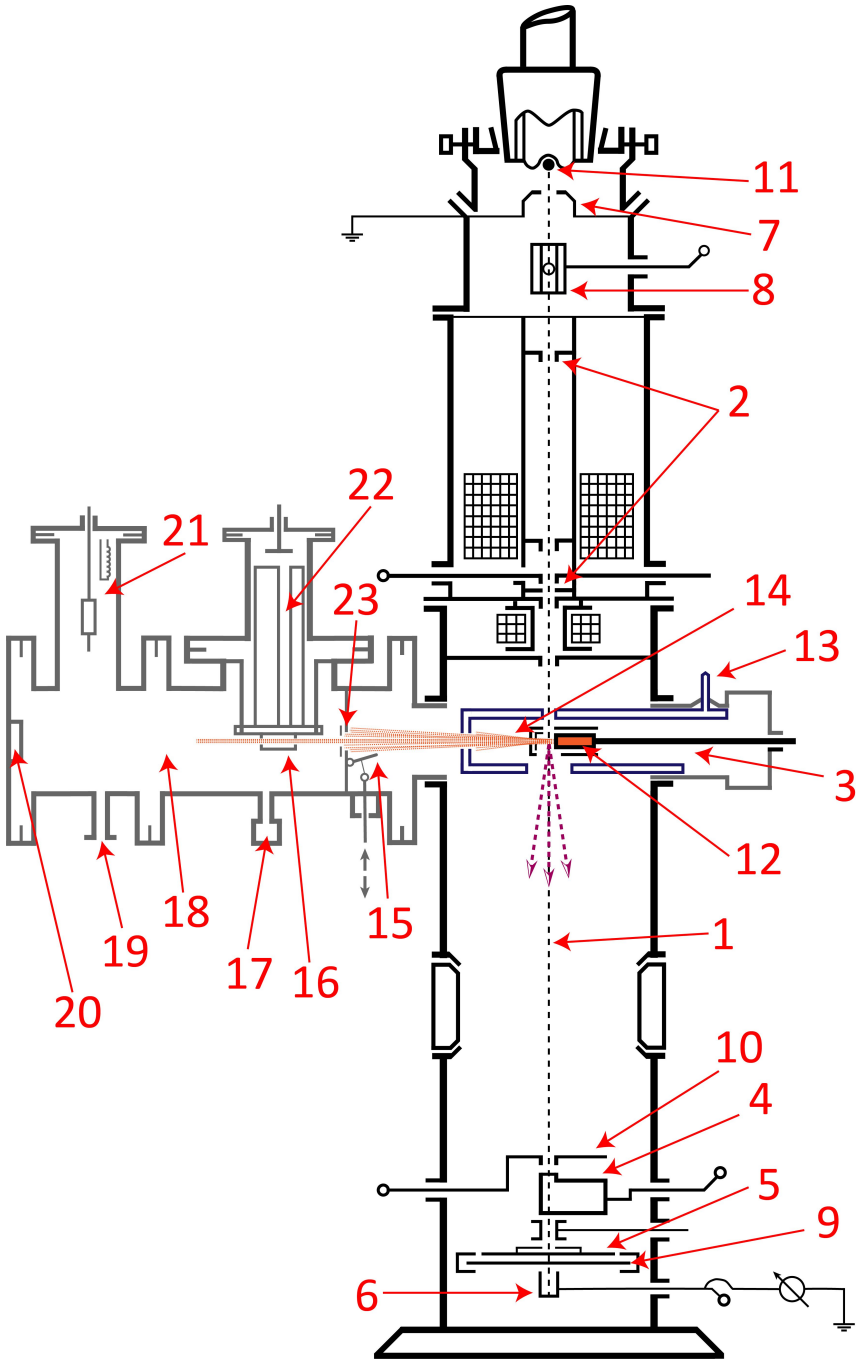


1 – electron beam, 2 - diaphragms, 3 - evaporator-reactor, 4 - trap for unscattered electrons, 5 - rotating sector, 6 - Faraday cylinder with a luminescent material applied to the inner surface (used for aligning the electron beam to the center of the sector), 7 - anode, 8 - electron beam gate, 9 - photographic plate, 10 - fluorescent screen, 11 - cathode, 12 - effusion cell, 13 - trap for collecting vapors of the substances under study, 14 - molecular beam, 15 - gate valve, 16 - ionization chamber, 17 - PMI-2 sensor, 18 - mass spectrometer unit, 19 - fore-vacuum pumping fitting, 20 - viewing window, 21 - orbitron hetero-ion pump, 22 - APDM-1 mass spectrometer monopolar detector, 23 - 9 mm diameter hole.

Figure S1: Scheme of the GED/MS experimental setup.

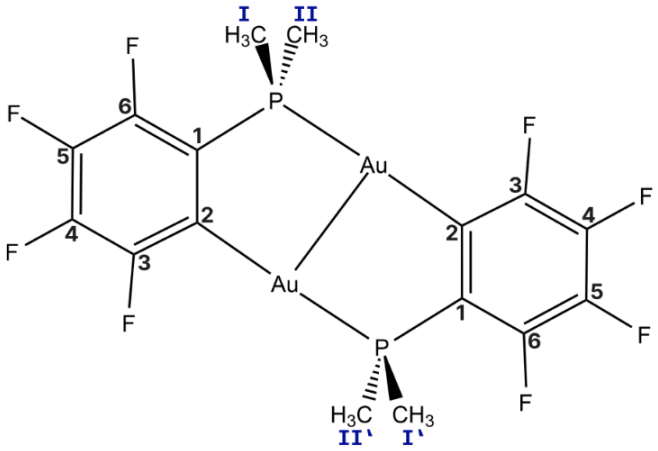


Figure S2: Atom numbering in **3** used in structure refinement.

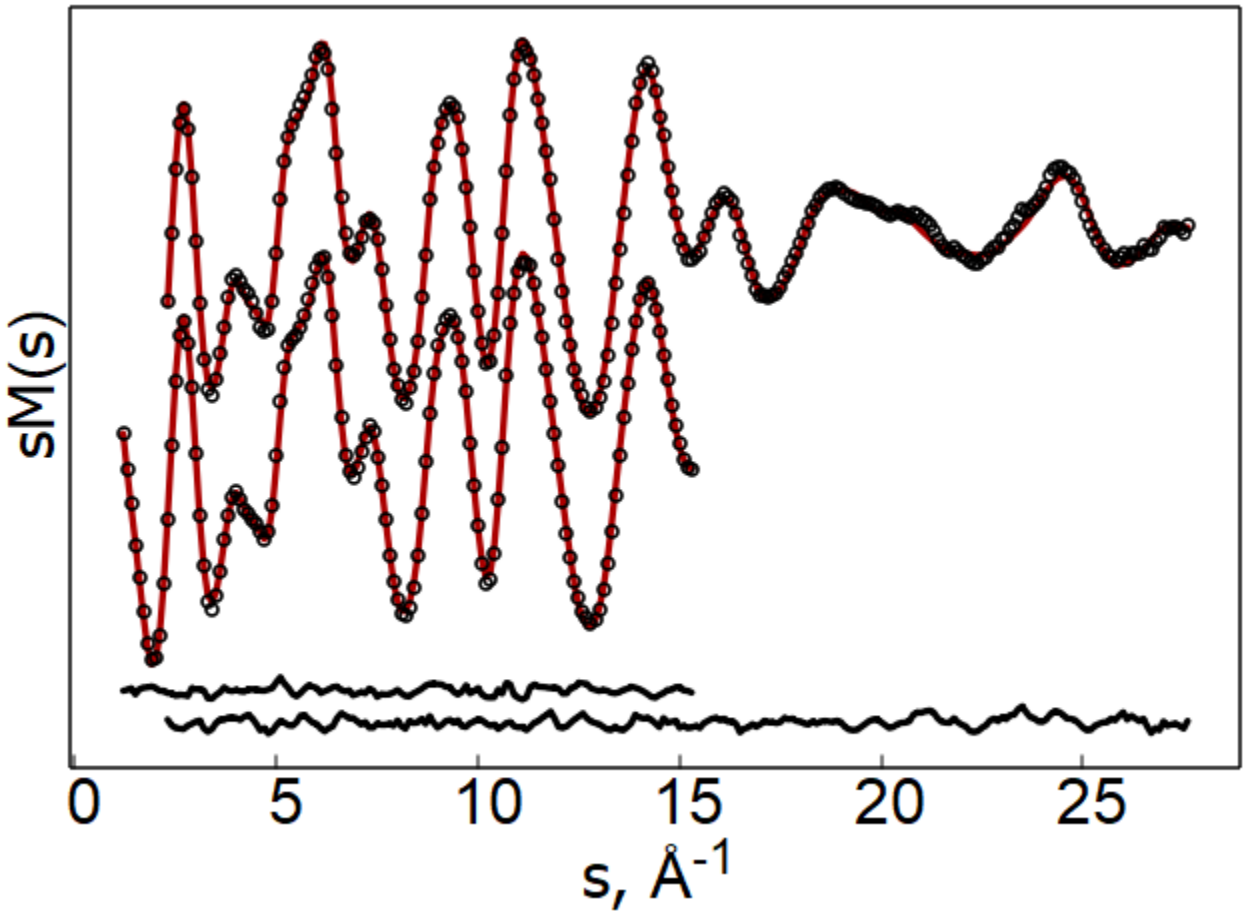


Figure S3: Experimental (circles) and model (solid lines) molecular intensities $sM(s)$ of **3** and respective residual curves $\Delta sM(s)$.

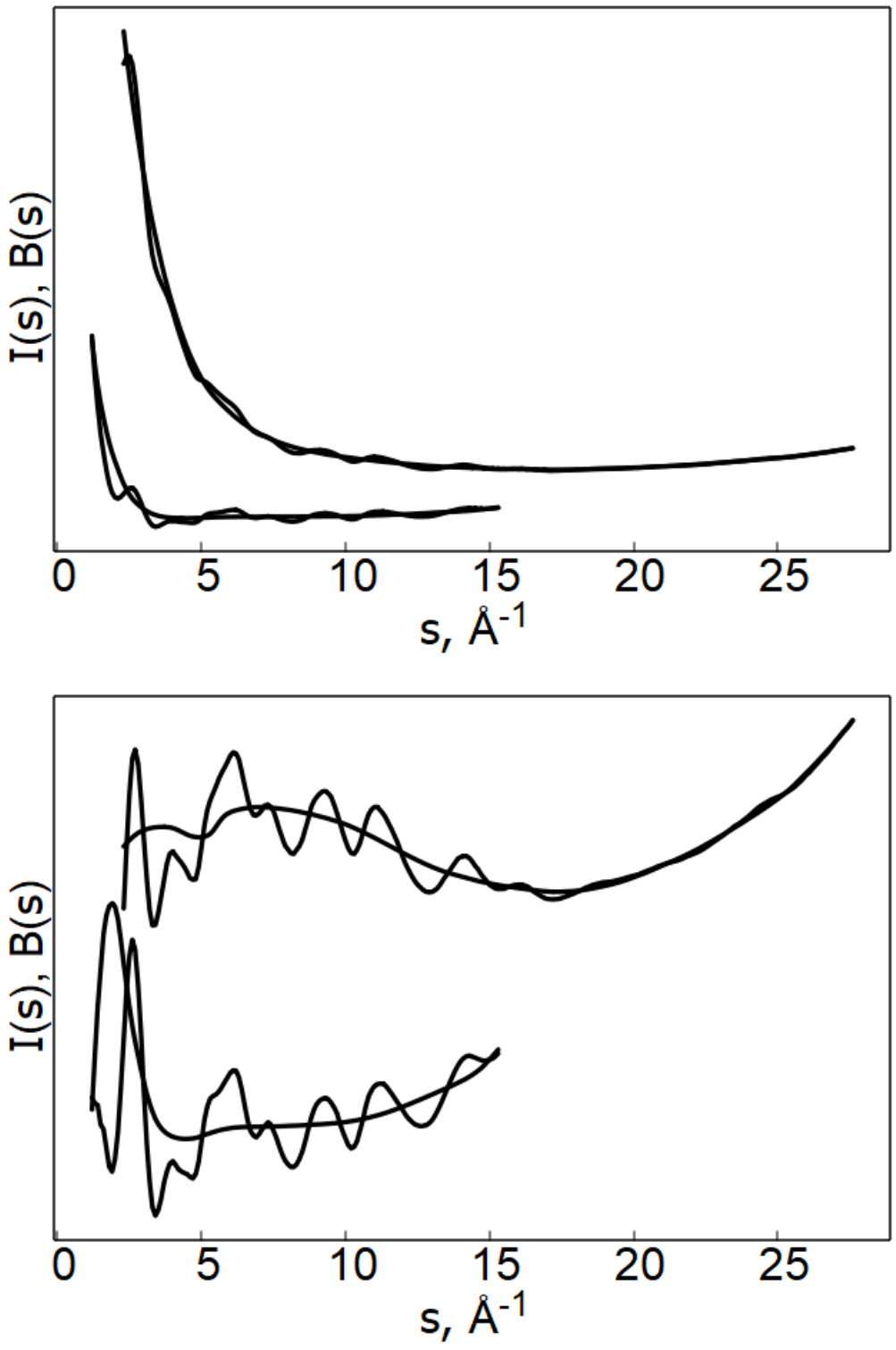


Figure S4: Original and reduced (by dividing by sigmoid function) total electron diffraction intensities of **3** and respective smoothed background lines.

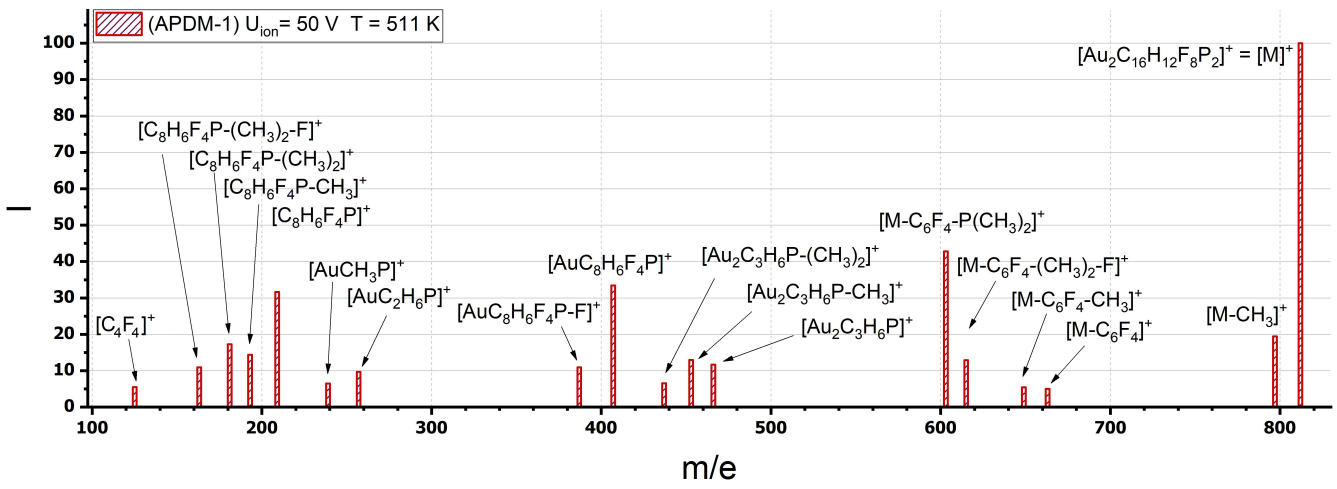


Figure S5: Mass spectra of **3** recorded during GED/MS experiments.

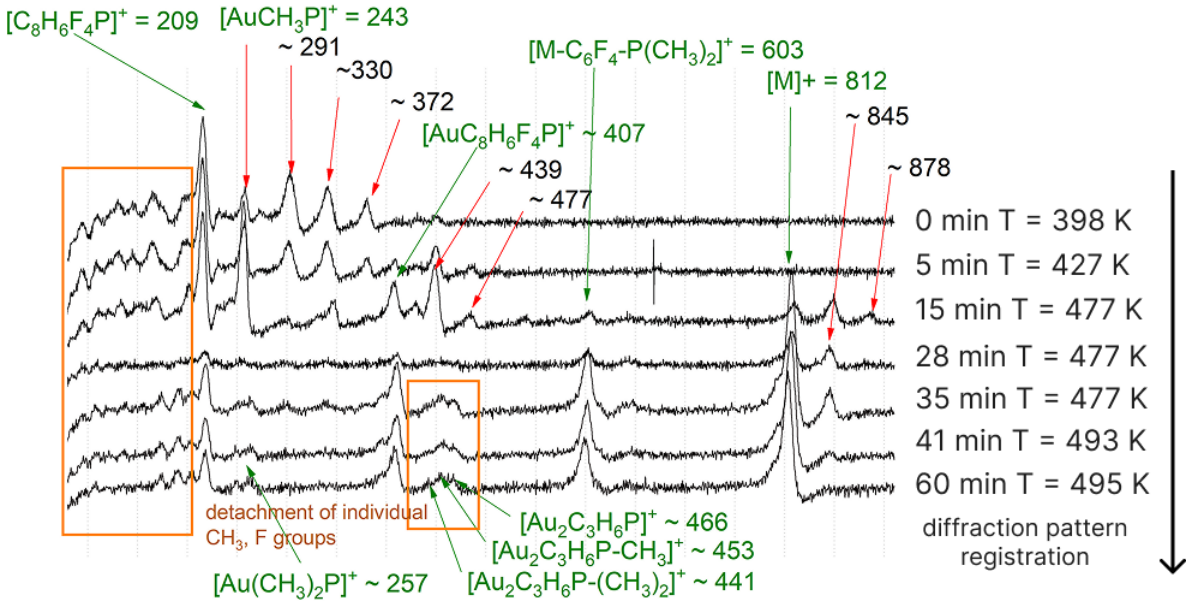


Figure S6: Evolution of mass spectrum of **3** at initial stages of GED/MS experiments before recording diffraction patterns.

# References


(1) Girichev, G. V.; Utkin, A. N.; Revichev, Y. F. Modernization of the EMR-100 Setup for the Studies of Gases. *Prib. Tekh. Eksp.* **1984**, *27*, 187–190.

(2) Girichev, G. V.; Shlykov, S. A.; Revichev, Y. F. Apparatus for Study of Molecular Structure of Valence-Unsaturated Compounds. *Prib. Tekh. Eksp.* **1986**, *29*, 167–169.

(3) Shlykov, S. A.; Girichev, G. V. A Radiofrequency Mass Spectrometer Based on APDM-1 Unit for the Mass Range of 1-1600 Amu. *Prib. Tekh. Eksp.* **1988**, *31*, 141–142.

(4) Bannwarth, C.; Ehlert, S.; Grimme, S. GFN2-xTB - An Accurate and Broadly Parametrized Self-Consistent Tight-Binding Quantum Chemical Method with Multipole Electrostatics and Density-Dependent Dispersion Contributions. *J. Chem. Theory Comput.* **2019**, *15*, 1652–1671.

(5) Pracht, P.; Bohle, F.; Grimme, S. Automated exploration of the low-energy chemical space with fast quantum chemical methods. *Phys. Chem. Chem. Phys.* **2020**, *22*, 7169–7192.

(6) Grimme, S. Exploration of Chemical Compound, Conformer, and Reaction Space with Meta-Dynamics Simulations Based on Tight-Binding Quantum Chemical Calculations. *J. Chem. Theory Comput.* **2019**, *15*, 2847–2862, PMID: 30943025.

(7) Pracht, P.; Grimme, S. CREST Version 2.10.2. 2020; `https://github.com/grimme-lab/crest/`.

(8) Vishnevskiy, Y. V. UNEX version 2.2. 2026; `https://unex.vishnevskiy.group`.

(9) Vishnevskiy, Y. V.; Zhabanov, Y. A. New implementation of the first-order perturbation theory for calculation of interatomic vibrational amplitudes and corrections in gas electron diffraction. *J. Phys. Conf. Ser.* **2015**, *633*, 012076.

(10) Sipachev, V. A. Calculation of shrinkage corrections in harmonic approximation. *J. Mol. Struct. (THEOCHEM)* **1985**, *121*, 143 – 151.

(11) Sipachev, V. A. The use of quantum-mechanical third-order force constants in structural studies. *J. Mol. Struct.* **2004**, *693*, 235 – 240.

(12) Litman, Y. et al. i-PI 3.0: A flexible and efficient framework for advanced atomistic simulations. *J. Chem. Phys.* **2024**, *161*, 062504.

(13) Ceriotti, M.; Manolopoulos, D. E. Efficient First-Principles Calculation of the Quantum Kinetic Energy and Momentum Distribution of Nuclei. *Phys. Rev. Lett.* **2012**, *109*, 100604.

(14) Vishnevskiy, Y. V.; Tikhonov, D. Quantum corrections to parameters of interatomic distance distributions in molecular dynamics simulations. *Theor. Chem. Acc.* **2016**, *135*, 88.

(15) Hartree, D. R. The Wave Mechanics of an Atom with a Non-Coulomb Central Field. Part I. Theory and Methods. *Math. Proc. Camb. Philos. Soc.* **1928**, *24*, 89–110.

(16) Fock, V. Näherungsmethode zur Lösung des quantenmechanischen Mehrkörperproblems. *Z. Physik* **1930**, *61*, 126–148.

(17) Adamo, C.; Barone, V. Toward reliable density functional methods without adjustable parameters: The PBE0 model. *J. Chem. Phys.* **1999**, *110*, 6158–6170.

(18) Grimme, S. Semiempirical hybrid density functional with perturbative second-order correlation. *J. Chem. Phys.* **2006**, *124*, 034108.

(19) Chai, J.-D.; Head-Gordon, M. Systematic optimization of long-range corrected hybrid density functionals. *J. Chem. Phys.* **2008**, *128*, 084106.

(20) Grimme, S.; Brandenburg, J. G.; Bannwarth, C.; Hansen, A. Consistent structures and interactions by density functional theory with small atomic orbital basis sets. *J. Chem. Phys.* **2015**, *143*, 054107.

(21) Grimme, S.; Hansen, A.; Ehlert, S.; Mewes, J.-M. r2SCAN-3c: A "Swiss army knife" composite electronic-structure method. *J. Chem. Phys.* **2021**, *154*, 064103.

(22) Møller, C.; Plesset, M. S. Note on an Approximation Treatment for Many-Electron Systems. *Phys. Rev.* **1934**, *46*, 618–622.

(23) Grimme, S. Improved second-order Møller–Plesset perturbation theory by separate scaling of parallel- and antiparallel-spin pair correlation energies. *J. Chem. Phys.* **2003**, *118*, 9095–9102.

(24) Neese, F. Software update: The ORCA program system—Version 5.0. *Wiley Interdiscip. Rev. Comput. Mol. Sci.* **2022**, *12*, e1606.

(25) Neese, F. The SHARK integral generation and digestion system. *J. Comput. Chem.* **2023**, *44*, 381–396.

(26) Weigend, F.; Ahlrichs, R. Balanced basis sets of split valence, triple zeta valence and quadruple zeta valence quality for H to Rn: Design and assessment of accuracy. *Phys. Chem. Chem. Phys.* **2005**, *7*, 3297–3305.

(27) Grimme, S.; Antony, J.; Ehrlich, S.; Krieg, H. A consistent and accurate ab initio parametrization of density functional dispersion correction (DFT-D) for the 94 elements H-Pu. *J. Chem. Phys.* **2010**, *132*, 154104.

(28) Grimme, S.; Ehrlich, S.; Goerigk, L. Effect of the damping function in dispersion corrected density functional theory. *J. Comput. Chem.* **2011**, *32*, 1456–1465.

(29) Caldeweyher, E.; Ehlert, S.; Hansen, A.; Neugebauer, H.; Spicher, S.; Bannwarth, C.;

Grimme, S. A generally applicable atomic-charge dependent London dispersion correction. *J. Chem. Phys.* **2019**, *150*, 154122.

(30) Neese, F.; Wennmohs, F.; Hansen, A.; Becker, U. Efficient, approximate and parallel Hartree–Fock and hybrid DFT calculations. A 'chain-of-spheres' algorithm for the Hartree–Fock exchange. *Chem. Phys.* **2009**, *356*, 98–109.

(31) Kossmann, S.; Neese, F. Efficient Structure Optimization with Second-Order Many-Body Perturbation Theory: The RIJCOSX-MP2 Method. *J. Chem. Theory Comput.* **2010**, *6*, 2325–2338.

(32) Helmich-Paris, B.; de Souza, B.; Neese, F.; Izsák, R. An improved chain of spheres for exchange algorithm. *J. Chem. Phys.* **2021**, *155*, 104109.

(33) Filatov, M.; Cremer, D. Representation of the exact relativistic electronic Hamiltonian within the regular approximation. *J. Chem. Phys.* **2003**, *119*, 11526–11540.

(34) Kutzelnigg, W.; Liu, W. Quasirelativistic theory equivalent to fully relativistic theory. *J. Chem. Phys.* **2005**, *123*, 241102.

(35) Franzke, Y. J.; Spiske, L.; Pollak, P.; Weigend, F. Segmented Contracted Error-Consistent Basis Sets of Quadruple-zeta Valence Quality for One- and Two-Component Relativistic All-Electron Calculations. *J. Chem. Theory Comput.* **2020**, *16*, 5658–5674.

(36) Lee, C.; Yang, W.; Parr, R. G. Development of the Colle-Salvetti correlation-energy formula into a functional of the electron density. *Phys. Rev. B* **1988**, *37*, 785–789.

(37) Becke, A. D. Density-functional thermochemistry. III. The role of exact exchange. *The Journal of Chemical Physics* **1993**, *98*, 5648–5652.

(38) Grimme, S. Semiempirical GGA-type density functional constructed with a long-range dispersion correction. *J. Comput. Chem.* **2006**, *27*, 1787–1799.

(39) Schmider, H. L.; Becke, A. D. Optimized density functionals from the extended G2 test set. *J. Chem. Phys.* **1998**, *108*, 9624–9631.

(40) Boese, A. D.; Martin, J. M. L. Development of density functionals for thermochemical kinetics. *J. Chem. Phys.* **2004**, *121*, 3405–3416.

(41) Perdew, J. P.; Burke, K.; Ernzerhof, M. Generalized Gradient Approximation Made Simple. *Phys. Rev. Lett.* **1997**, *78*, 1396–1396.

(42) Perdew, J. P. Density-functional approximation for the correlation energy of the inhomogeneous electron gas. *Phys. Rev. B* **1986**, *33*, 8822–8824.

(43) Becke, A. D. Density-functional exchange-energy approximation with correct asymptotic behavior. *Phys. Rev. A* **1988**, *38*, 3098–3100.

(44) Yanai, T.; Tew, D. P.; Handy, N. C. A new hybrid exchange–correlation functional using the Coulomb-attenuating method (CAM-B3LYP). *Chem. Phys. Lett.* **2004**, *393*, 51–57.

(45) Vydrov, O. A.; Scuseria, G. E. Assessment of a long-range corrected hybrid functional. *J. Chem. Phys.* **2006**, *125*, 234109.

(46) Vydrov, O. A.; Scuseria, G. E.; Perdew, J. P. Tests of functionals for systems with fractional electron number. *J. Chem. Phys.* **2007**, *126*, 154109.

(47) Vydrov, O. A.; Heyd, J.; Krukau, A. V.; Scuseria, G. E. Importance of short-range versus long-range Hartree-Fock exchange for the performance of hybrid density functionals. *J. Chem. Phys.* **2006**, *125*, 074106.

(48) Zhao, Y.; Schultz, N. E.; Truhlar, D. G. Exchange-correlation functional with broad accuracy for metallic and nonmetallic compounds, kinetics, and noncovalent interactions. *J. Chem. Phys.* **2005**, *123*, 161103.

(49) Zhao, Y.; Truhlar, D. G. The M06 suite of density functionals for main group thermochemistry, thermochemical kinetics, noncovalent interactions, excited states, and transition elements: two new functionals and systematic testing of four M06-class functionals and 12 other functionals. *Theor Chem Account* **2008**, *120*, 215–241.

(50) Zhao, Y.; Truhlar, D. G. Comparative DFT Study of van der Waals Complexes: Rare-Gas Dimers, Alkaline-Earth Dimers, Zinc Dimer, and Zinc-Rare-Gas Dimers. *J. Phys. Chem. A* **2006**, *110*, 5121–5129.

(51) Zhao, Y.; Truhlar, D. G. Density Functional for Spectroscopy: No Long-Range Self-Interaction Error, Good Performance for Rydberg and Charge-Transfer States, and Better Performance on Average than B3LYP for Ground States. *J. Phys. Chem. A* **2006**, *110*, 13126–13130.

(52) Adamo, C.; Barone, V. Toward reliable density functional methods without adjustable parameters: The PBE0 model. *J. Chem. Phys.* **1999**, *110*, 6158–6170.

(53) Tao, J.; Perdew, J. P.; Staroverov, V. N.; Scuseria, G. E. Climbing the Density Functional Ladder: Nonempirical Meta–Generalized Gradient Approximation Designed for Molecules and Solids. *Phys. Rev. Lett.* **2003**, *91*, 146401.

(54) Staroverov, V. N.; Scuseria, G. E.; Tao, J.; Perdew, J. P. Erratum: Comparative assessment of a new nonempirical density functional: Molecules and hydrogen-bonded complexes. *J. Chem. Phys.* **2004**, *121*, 11507–11507.

(55) Van Voorhis, T.; Scuseria, G. E. A novel form for the exchange-correlation energy functional. *J. Chem. Phys.* **1998**, *109*, 400–410.

(56) Xu, X.; Goddard, W. A. The X3LYP extended density functional for accurate descriptions of nonbond interactions, spin states, and thermochemical properties. *Proc. Natl. Acad. Sci. U.S.A.* **2004**, *101*, 2673–2677.

(57) Frisch, M.; Trucks, G.; Schlegel, H.; Scuseria, G.; Robb, M.; Cheeseman, J.; Scalmani, G.; Barone, V.; Mennucci, B.; Petersson, G. Gaussian09. 2009.

(58) Dunning, T. H. Gaussian basis sets for use in correlated molecular calculations. I. The atoms boron through neon and hydrogen. *J. Chem. Phys.* **1989**, *90*, 1007–1023.

(59) Woon, D. E.; Dunning, T. H. Gaussian basis sets for use in correlated molecular calculations. III. The atoms aluminum through argon. *J. Chem. Phys.* **1993**, *98*, 1358–1371.

(60) Andrae, D.; Haeussermann, U.; Dolg, M.; Stoll, H.; Preuss, H. Energy-adjustedab initio pseudopotentials for the second and third row transition elements. *Theoret. Chim. Acta* **1990**, *77*, 123–141.

(61) Schwerdtfeger, P.; Dolg, M.; Schwarz, W. H. E.; Bowmaker, G. A.; Boyd, P. D. W. Relativistic effects in gold chemistry. I. Diatomic gold compounds. *J. Chem. Phys.* **1989**, *91*, 1762–1774.

(62) Pritchard, B. P.; Altarawy, D.; Didier, B.; Gibson, T. D.; Windus, T. L. New Basis Set Exchange: An Open, Up-to-Date Resource for the Molecular Sciences Community. *J. Chem. Inf. Model.* **2019**, *59*, 4814–4820.

(63) Nagy, P. R.; Kállay, M. Approaching the Basis Set Limit of CCSD(T) Energies for Large Molecules with Local Natural Orbital Coupled-Cluster Methods. *J. Chem. Theory Comput.* **2019**, *15*, 5275–5298.

(64) Nagy, P. R. State-of-the-art local correlation methods enable affordable gold standard quantum chemistry for up to hundreds of atoms. *Chem. Sci.* **2024**, *15*, 14556–14584.

(65) Kállay, M. et al. The MRCC program system: Accurate quantum chemistry from water to proteins. *J. Chem. Phys.* **2020**, *152*, 074107.

(66) Figgen, D.; Rauhut, G.; Dolg, M.; Stoll, H. Energy-consistent pseudopotentials for

group 11 and 12 atoms: adjustment to multi-configuration Dirac–Hartree–Fock data. *Chem. Phys.* **2005**, *311*, 227–244.

(67) Peterson, K. A.; Puzzarini, C. Systematically convergent basis sets for transition metals. II. Pseudopotential-based correlation consistent basis sets for the group 11 (Cu, Ag, Au) and 12 (Zn, Cd, Hg) elements. *Theor. Chem. Acc.* **2005**, *114*, 283–296.

(68) Dunning, T. H. Gaussian basis sets for use in correlated molecular calculations. I. The atoms boron through neon and hydrogen. *J. Chem. Phys.* **1989**, *90*, 1007–1023.

(69) Woon, D. E.; Thom H. Dunning, J. Gaussian basis sets for use in correlated molecular calculations. III. The atoms aluminum through argon. *J. Chem. Phys.* **1993**, *98*, 1358–1371.

(70) Hill, J. G.; Peterson, K. A. Explicitly Correlated Coupled Cluster Calculations for Molecules Containing Group 11 (Cu, Ag, Au) and 12 (Zn, Cd, Hg) Elements: Optimized Complementary Auxiliary Basis Sets for Valence and Core–Valence Basis Sets. *J. Chem. Theory Comput.* **2012**, *8*, 518–526.

(71) Stoychev, G. L.; Auer, A. A.; Neese, F. Automatic Generation of Auxiliary Basis Sets. *J. Chem. Theory Comput.* **2017**, *13*, 554–562.